ГЛАСНИК Српског географског друштва 105(2) 157-174
BULLETIN OF THE SERBIAN GEOGRAPHICAL SOCIETY 2025

Original scientific paper

UDC 551.444:[007:912]:004](65)
https://doi.org/10.2298/GSGD2502157T

Received: April 4, 2025
Corrected: June 9, 2025
Accepted: June 26, 2025

Mohammed Tiaiba[1]*, Belkacem Merzouk, Sofiane Bensefia*, Toufik Herizi***

** Environment and Health Laboratory, Department of Agricultural Sciences, Faculty of Life and Natural Sciences and Earth and Universe Sciences, Mohamed El-Bachir El-Ibrahimi University, Bordj Bou Arreridj 34000, Algeria*
*** Laboratory of Water, Environment and Renewable Energies, Department of Hydraulics, Faculty of Technology, University of M'sila, University pole, Road Bordj Bou Arreridj, M'sila 28000, Algeria*

GROUNDWATER QUALITY ASSESSMENT USING SPATIO-TEMPORAL EVOLUTION OF WATER QUALITY INDEX AND GIS IN K'SOB WATERSHED (SEMIARID AREA—EAST ALGERIA)

Abstract: Groundwater is a crucial natural resource, particularly in arid and semi-arid regions, where it serves as a primary source for drinking and irrigation. The K'sob watershed in Algeria is significant for its groundwater resources. This study aims to assess the groundwater quality of the K'sob aquifer and investigate the spatial distribution of quality parameters to identify areas with the best drinking water quality. The study combines the Water Quality Index (WQI) and Geographic Information System (GIS) methodologies. Twenty groundwater samples were collected and analyzed for major cations and anions. Spatial distribution maps of parameters including pH, temperature (T°), electrical conductivity (EC), total hardness (TH), turbidity, total alkalinity (TAC), chloride (Cl-), nitrate (NO3-), bicarbonate (HCO3-), calcium (Ca2+), and magnesium (Mg2+) were created using the Inverse Distance Weighted (IDW) interpolation method in a GIS environment. The WQI results revealed temporal variations in groundwater quality between 2022 and 2024. In 2022, 5% of samples were of excellent quality, 60% good quality, 15% poor quality, 5% very poor quality, and 15% unsuitable for drinking purposes. By 2024, samples classified as excellent quality increased to 25%, while good quality samples decreased to 35%. Poor quality samples remained stable at 15%, very poor quality samples increased to 10%, and those unsuitable for drinking remained at 15%. This research demonstrates the effective combination of GIS and WQI in assessing groundwater quality over space and time. The findings can support decision-makers in planning the operation and management of groundwater resources.

Keywords: groundwater, spatio-temporal evolution, GIS, IDW, WQI

[1] mohamed.tiaiba@univ-bba.dz (corresponding author)
Mohammed Tiaiba (https://orcid.org/0009-0000-3755-1226)
Belkacem Merzouk (https://orcid.org/0000-0003-1877-922X)
Sofiane Bensefia (https://orcid.org/0000-0001-8040-2111)
Toufik Herizi (https://orcid.org/0009-0000-3809-8339)

Introduction

Groundwater quality represents a significant environmental challenge worldwide, particularly in arid and semi-arid regions where it constitutes the primary water resource (Umar et al., 2009). The chemical composition and quality of groundwater are governed by complex interactions of hydrogeological factors, including recharge mechanisms, precipitation patterns, and geochemical processes within aquifer systems. The deterioration of water quality through pollution poses multifaceted threats to human health, economic development, and societal well-being (Milovanovic, 2007).

In the Algerian context, groundwater resources are critical components of the national water supply infrastructure, serving dual strategic functions in providing essential municipal drinking water and supporting extensive agricultural activities. However, intensive exploitation has resulted in significant aquifer depletion and quality deterioration, emphasizing the need for comprehensive quality assessments (Bourmada et al., 2024).

Recent advances in hydrogeological research have led to the widespread adoption of Geographic Information System (GIS) methodologies and Water Quality Index (WQI) assessments. The WQI, initially developed by Brown et al. (1970), has emerged as a fundamental tool in groundwater quality assessment, while GIS-based approaches have demonstrated remarkable efficacy in analyzing spatial patterns of water resources (Kanagaraj et al. 2019). Recent studies have demonstrated the effectiveness of combining these approaches. Sadat-Noori et al. (2014) integrated WQI with GIS techniques in Iran's Saveh-Nobaran aquifer, while Ali et al. (2024) employed both WQI and Principal Component Analysis in India's Achhnera block.

Despite these advances, no comprehensive studies have employed this integrated technique in the K'sob aquifer, Algeria, despite the region facing increasing anthropogenic pressures from population growth, industrial expansion, and agricultural intensification. The present study addresses this gap by evaluating the groundwater quality status of the K'sob aquifer through an integrated methodological approach combining conventional hydrochemical analysis with GIS techniques to develop a comprehensive spatio-temporal evolution of the Water Quality Index map.

This novel approach provides a systematic monitoring framework for groundwater quality assessment, enabling spatial identification of water quality variations with respect to drinking water suitability. The study utilizes previously unpublished hydrochemical data to generate spatially referenced quality indices, facilitating improved understanding of groundwater quality distribution patterns and providing an accessible decision-support tool for diverse stakeholders.

Materials and Methods

Study area

The K'sob watershed, located in the great Hodna basin in northern Algeria, drains an area of 1481 km² and is situated entirely in the province of Bordj Bou Arréridj (BBA) in eastern Algeria. It is located between 4°34′37″E and 5°06′09″E longitude and 35°33′52″N and 36°18′45″N latitude. The K'sob watershed is characterized by rugged and varied terrain with nearby mountains and a wide plateau in the center. Maximum and minimum elevations are 1,887 and 590 m, respectively (Figure 1).

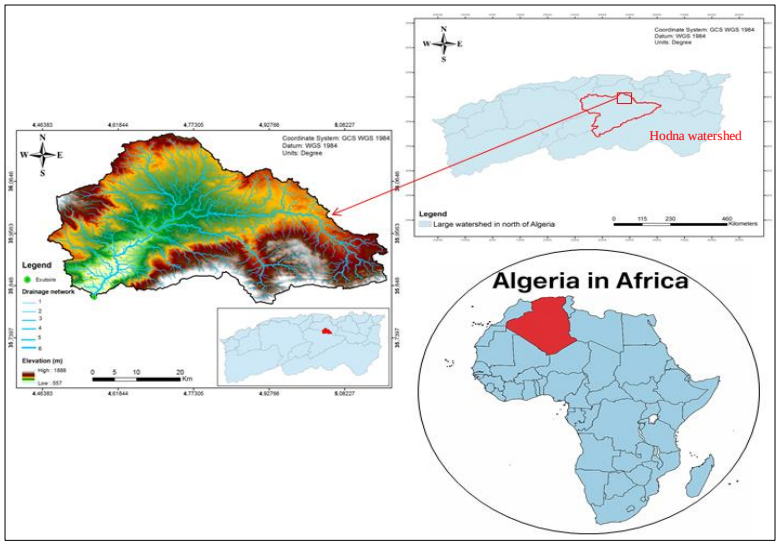

Fig. 1. The location of the study area

Geological and hydrogeological set-up

The geological framework of the K'sob watershed displays is characterized by diverse lithological compositions and differential susceptibility to erosion (Figure 2). The northern and central portions of the basin, comprises predominantly of easily erodible formations including Quaternary alluvial terraces, clays, Miocene marls, and sandstones that are continuously subjected to intensive mechanical erosion processes. In contrast, the southern part of the basin, consists of resistant carbonate formations dominated by limestone and dolomite. The stratigraphic sequence spans from Triassic gypsic clays to Quaternary formations comprising scree deposits and alluvium.

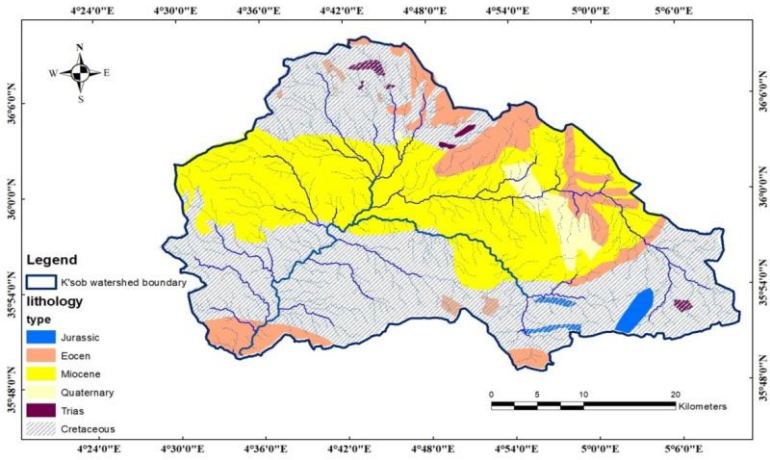

Fig. 2. Lithology map of the K'sob watershed. Quaternary formations (scree deposits and alluvium); Miocene (clays and marls sandstones); Eocene (limestone and marls); Cretaceous (marly limestone and dolomites); Jurassic (limestone), Trias (gyspsic clay)

Hydrogeological investigations were conducted using 20 monitoring wells (S1-S20) strategically distributed across the watershed to capture spatial variations in groundwater conditions. For each monitoring point, geographic coordinates, ground surface elevation, static water level depth, hydraulic head calculations, and operational status were measured and recorded (Table 1). A comprehensive hydraulic head distribution map was constructed using measurements from the monitoring network, with isopiezometric contours interpolated to represent equal hydraulic head values. The spatial distribution of hydraulic heads reveals nine distinct classes ranging from 520-583 m to 1025-1087 m above sea level, as illustrated in the hydraulic head map (Figure 3).

Table 1. Characteristics piezometric of water points in the K'sob watershed

Well ID	Coordinates		Elevation (m asl)	Static Water Level (m)	Hydraulic Head (m asl)	Operational Status
	Longitude	Latitude				
S1	4,884°E	35,901°N	1113	110	1013	Active
S2	4,886°E	35,919°N	1024	100	894	Active
S3	4,885°E	35,917°N	1030	100	905	Active
S4	4,899°E	35,866°N	1188	220	1068	Active
S5	4,915°E	35,866°N	1162	180	1052	Active
S6	4,890°E	35,917°N	1040	150	940	Active
S7	4,913°E	35,854°N	1175	200	1025	Active
S8	5,043°E	35,916°N	1187	250	1087	Active
S9	5,029°E	35,928°N	1160	230	1050	Active
S10	4,976°E	35,976°N	1040	130	975	Active
S11	4,968°E	36,050°N	1040	150	950	Active
S12	4,931°E	35,965°N	1060	150	910	Active
S13	4,818°E	36,044°N	980	120	860	Active
S14	4,617°E	36,025°N	980	125	855	Active
S15	4,642°E	36,123°N	1113	190	923	Active
S16	4,738°E	36,094°N	1040	130	910	Active
S17	4,783°E	35,970°N	920	110	810	Active
S18	4,552°E	35,947°N	650	100	550	Active
S19	4,544°E	35,888°N	600	80	580	Active
S20	4,644°E	35,907°N	620	100	520	Active

The hydraulic head analysis reveals a dominant groundwater flow direction from east/northeast toward west/southwest, as indicated by the flow direction arrows on the hydraulic head map. The groundwater flow pattern follows a trajectory parallel to the surface drainage network. Primary recharge zones are identified in the eastern and northeastern sectors, characterized by the highest hydraulic head values (1025-1087 m above sea level, represented in light pink), while the principal discharge area is located in the southwestern region with the lowest values (520-583 m above sea level, shown in dark green). Spatial analysis of isopiezometric contour spacing indicates significant heterogeneity in aquifer hydraulic properties. Narrow contour spacing spacing in the northern region suggests lower transmissivity, whereas wider spacing in the southwest indicates higher hydraulic conductivity, associated with the more permeable carbonate formations. Localized depression cones observed around monitoring points S18, S19, and S20 in the southwestern discharge

zone, as well as around points S7 and S9 in the central-eastern area, indicate either intensive groundwater extraction zones or hydrogeological discontinuities linked to lithological transitions. The hydrogeological analysis integrates geological mapping, piezometric monitoring, topographic data, and surface drainage network analysis to ensure coherence between observed groundwater flow directions and surface water drainage patterns, validating the conceptual hydrogeological model developed for the K'sob watershed.

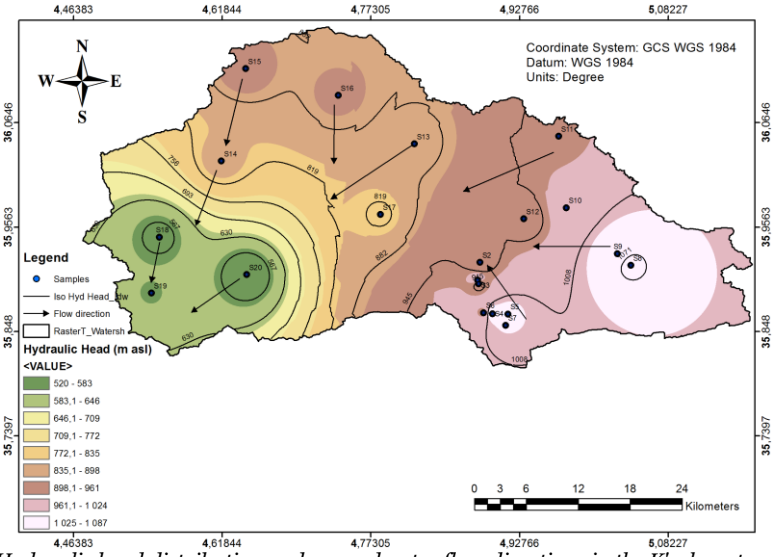

Fig. 3. Hydraulic head distribution and groundwater flow directions in the K'sob watershed

Sampling and Analysis

Groundwater samples were collected from twenty monitoring wells distributed across the K'sob watershed in February 2022. Prior to sampling, each well was purged to ensure representative groundwater samples. Samples were collected in sterilized 1000 ml plastic containers and preserved in airtight ice-cold containers during transport to the laboratory for detailed analysis of various physicochemical parameters using standard methods (APHA, 2005).

Physical parameters including hydrogen ion concentration (pH), temperature (T°), electrical conductivity (EC), and turbidity were measured in situ at 25°C using a handheld digital pH/EC/TDS/turbidity meter (HannaHI-9829). Chemical analyses for total hardness (TH), total alkalinity (TAC), chloride (Cl^-), bicarbonate (HCO_3^-), calcium (Ca^{2+}), magnesium (Mg^{2+}), and nitrate (NO_3^-) were performed following standard procedures at the certified Algerian Water Laboratory (A.D.E.) of Bordj Bou Arréridj. These parameters were selected based on expert opinion, data availability, and their importance in assessing groundwater quality. Previous studies have also utilized these water quality parameters for examining groundwater quality trends in different regions worldwide (Masood et al. 2022; Piyathilake et al. 2022).

Water Quality Index method

The Water Quality Index (WQI) is a standardized methodology that quantifies the cumulative impact of multiple water quality parameters on overall water quality, particularly for human consumption assessment. This analytical approach transforms complex water quality data into a single numerical value, facilitating comprehensive evaluation of water potability. The calculation of WQI incorporates the Algerian drinking water standard (2014) and the World Health Organization (WHO, 2017) drinking water standards as reference values. The methodology assigns parameter weightages inversely proportional to their respective WHO-recommended standard values, reflecting the relative significance of each parameter in determining water quality (Mishra and Patel, 2001; Naik and Purohit, 2001).

The WQI calculation methodology comprises three distinct stages. In the first stage, relative weights (wi) were assigned to eleven physicochemical parameters (pH, T°, EC, TH, turbidity, TAC, Cl^-, NO_3^-, HCO_3^-, Ca^{2+}, and Mg^{2+}) based on their potential impact on human health (Table 2).

In the weighting scheme, nitrate was assigned the maximum weight of 5, reflecting its critical significance in water quality assessment (Srinivasamoorthy et al., 2008). Conversely, bicarbonate received the minimum weight of 1 due to its relatively minor influence on overall water quality. Intermediate weights between 1 and 5 were allocated to other ionic parameters based on their relative contributions to drinking water quality (Ketata-Rokbani et al., 2011).

In the second stage, the relative weight (Wi) of each parameter is computed using:

$$Wi = wi / \Sigma^{n}_{i=1} wi \quad (1)$$

where wi is the weight of each parameter, n is the number of parameters, and Wi is the relative weight. The weight (wi), calculated relative weight (Wi) values, and WHO standards for each parameter are presented in Table 2.

In the third stage, a quality rating scale (qi) is calculated for each parameter using:

$$qi = (Ci/Si) \times 100 \quad (2)$$

where qi is the quality rating, Ci is the concentration of each chemical parameter (mg/L), and Si is the WHO standard for each chemical parameter (mg/L).

For computing the WQI, the SI is first determined for each chemical parameter using:

$$SIi = Wi \times qi$$

$$WQI = \Sigma^{n}_{i=1} SIi \quad (3)$$

where SIi is the sub-index of *i*th parameter, q_i is the rating based on concentration of *i*th parameter, and n is the number of parameters.

Table 2. The weight (wi) and relative weight (Wi) of each chemical parameter

Parameter	Drinking-water standards		Weight (wi)	Relative weight (Wi)
	Algerian [2014]	WHO [2017]		
pH	≥ 6,5 et ≤ 9	7 – 8	3	0,091
T (°C)	25	–	2	0,061
EC (µS/cm)	2800 at 20 °C	–	3	0,091
TH as $CaCO_3$ (mg/L)	500	200	3	0,091
Turbidity (NTU)	5	–	3	0,091
TAC as $CaCO_3$ (mg/L)	65	–	3	0,091
Cl^- (mg/L)	500	250	4	0,121
NO_3^- (mg/L)	50	50	5	0,152
HCO_3^- (mg/L)	–	–	1	0,030
Ca^{2+} (mg/L)	200	100 – 300	3	0,091
Mg^{2+} (mg/L)	–	–	3	0,091
			$\sum Wi = 33$	$\sum W_i = 1$

The calculated WQI values are categorized into five distinct classes (Table 3): excellent, good, poor, very poor, and unsuitable for human consumption (Brown et al., 1972; Chatterjee and Raziuddin., 2002; Fentie et al., 2024). This classification methodology has been extensively documented in recent literature (Adil Masood et al., 2022; Piyathilake et al., 2022; Arjun Ram et al., 2021; Ali Chabuk et al., 2020, Faraji et al., 2024; Bahrami et al., 2024).

Table 3. Classification of water quality and status based on weighted arithmetic WQI Method

WQI range	Type of groundwater
< 50	Excellent water
50 – 100	Good water
101 – 200	Poor water
201 – 300	Very poor water
> 300	Unsuitable for drinking purpose

GIS application

Geographic Information System (GIS) has emerged as a powerful tool for storing, analyzing, and displaying spatial data, facilitating evidence-based decision-making across engineering and environmental disciplines (Lo and Yeung, 2003; Sadat-Noori et al., 2014).

The spatiotemporal distribution of groundwater quality parameters was analyzed using ArcMap™ 10.3 software. Spatial interpolation was performed using the Inverse Distance Weighted (IDW) method with a power parameter of 2, selected for its demonstrated accuracy in hydrogeological applications. This methodology enabled the generation of high-resolution spatial distribution maps for all measured water quality parameters.

The IDW interpolation method estimates values at unsampled points using a weighted average of observed values at surrounding points, where the weights are inversely proportional to the distance from the interpolation location (Webster and Oliver, 2007). The general equation of the IDW estimator is expressed as:

$$Z(x_0) = \Sigma^{n}_{i=1} \lambda_i Z(x_i) \quad (4)$$

With:

$$\lambda_i = d_i^{-p} / \Sigma^{n}_{j=1}\, d_j^{-p} \quad (5)$$

where $Z(x_0)$ is the predicted value at the unsampled location x_0, $Z(x_i)$ is the observed value at the sampled location x_i, λ_i is the weight assigned to each observed value, d_i is the distance between x_0 and x_i, p is the power parameter (typically p = 2), and n is the number of sampled points used for estimation.

The power parameter p controls the influence of distant points on the interpolated values (Lu and Wong, 2008; Chen and Liu, 2012). Higher values of p result in greater influence from nearby points, while lower values yield a smoother interpolation surface (Shepard, 1968; ESRI, 2018).

Results and Discussion

This study analyzes eleven groundwater quality parameters collected in February 2022: pH, T°, EC, TH, turbidity, TAC, Cl^-, NO_3^-, HCO_3^-, Ca^{+2}, and Mg^{+2}. These parameters were evaluated using statistical measures, including minimum, maximum, mean, and standard deviation. The results are presented in Table 4 and accompanying spatial distribution maps.

Table 4. Statistical analysis of physical and chemical groundwater quality parameters

Parameter	Unit	Minimum	Maximum	Mean	Standard division
pH		6,63	8,00	7,37	0,32
T°	°C	13,90	21,60	17,88	2,05
EC	µs/cm	696	1855	961,80	385,70
TH	mg/l	218,10	640	429,28	107,57
Turbidity	NTU	0,41	19,80	2,77	4,96
TAC	mg/L	151	395	261,53	48,50
Cl^-	mg/L	40,90	163,58	87,20	38,44
NO_3^-	mg/L	1,30	58,90	17,95	15,78
HCO_3^-	mg/L	97,06	488,90	298,16	80,62
Ca^{+2}	mg/L	23,52	144	101,03	29,19
Mg^{+2}	mg/L	27,28	68,04	43,05	14,18

The statistical analysis of groundwater quality parameters reveals significant variations across the K'sob watershed (Table 4), with spatial distribution maps (Figure 4) providing valuable insights into the geographic patterns and hydrogeochemical processes affecting water quality. pH values indicate slightly alkaline conditions (mean: 7.37 ± 0.32), with all samples falling within the permissible range (6.5-9) according to Algerian Drinking-water Standards 2014, showing relatively uniform spatial distribution across most of the watershed with slightly higher alkaline values concentrated in the central and eastern portions. This spatial pattern suggests consistent lithological influences and limited anthropogenic impacts on pH buffering capacity throughout the study area (Sadat-Noori et al. 2014). Groundwater temperatures remain moderate and within acceptable ranges for drinking water quality, ranging from 13.90°C to 21.60°C with a mean of 17.88°C, exhibiting a clear spatial gradient with cooler temperatures in upstream/highland areas and progressively

warmer conditions in downstream/lowland regions, reflecting typical topographic and hydrogeological controls.

Electrical conductivity (EC), which indicates dissolved constituents concentration (Chaurasia et al. 2018), remained below regulatory limits (2800 µS/cm) across all sampling locations with values ranging from 696 to 1855 µS/cm, while the spatial distribution reveals significant heterogeneity with notably higher conductivity values concentrated in the southern and southeastern portions of the watershed, indicating areas of increased mineral dissolution potentially related to specific geological formations or prolonged water-rock interactions.

Total hardness, influenced by multiple ions (Ravikumar et al. 2011), exceeds the recommended level of 250 mg/L in approximately 15% of samples, with elevated values primarily in the central and southern areas correlating with regions of higher EC values, suggesting common hydrogeochemical processes controlling both parameters, likely related to carbonate mineral dissolution and cation exchange processes in specific geological units.

Water turbidity, caused by suspended particles affecting light transmission, exceeded the 5 NTU threshold in 15% of samples with values ranging from 0.41 to 19.80 NTU, showing scattered high-value hotspots rather than continuous zones, indicating localized sources of suspended particles potentially from surface water infiltration or anthropogenic activities.

Alkalinity measurements reflect the water's capacity to neutralize acids, with values showing moderate buffering potential across the watershed (Appelo and Postma 2005).

Chloride concentrations remained below the acceptable limit of 500 mg/L at all locations, though elevated levels can impart a salty taste and increase corrosivity (Pius et al., 2012; Sadat-Noori et al., 2014).

Nitrate concentrations exceeded the maximum contaminant limit of 50 mg/L in 5% of samples (specifically at site S9), with the spatial distribution revealing this distinct hotspot in the central-eastern portion of the watershed, strongly suggesting localized agricultural influences, particularly intensive fertilizer application in the immediate vicinity of this sampling location.

Bicarbonate demonstrated considerable variation across the watershed, though this parameter generally plays a minor role in water pollution assessment (Ketata et al., 2011), while calcium and magnesium concentrations remained within acceptable ranges for drinking water quality, with both cations exhibiting similar spatial distributions with elevated concentrations in the central and southern watershed areas, reflecting the dissolution of carbonate minerals and natural hydrogeochemical evolution.

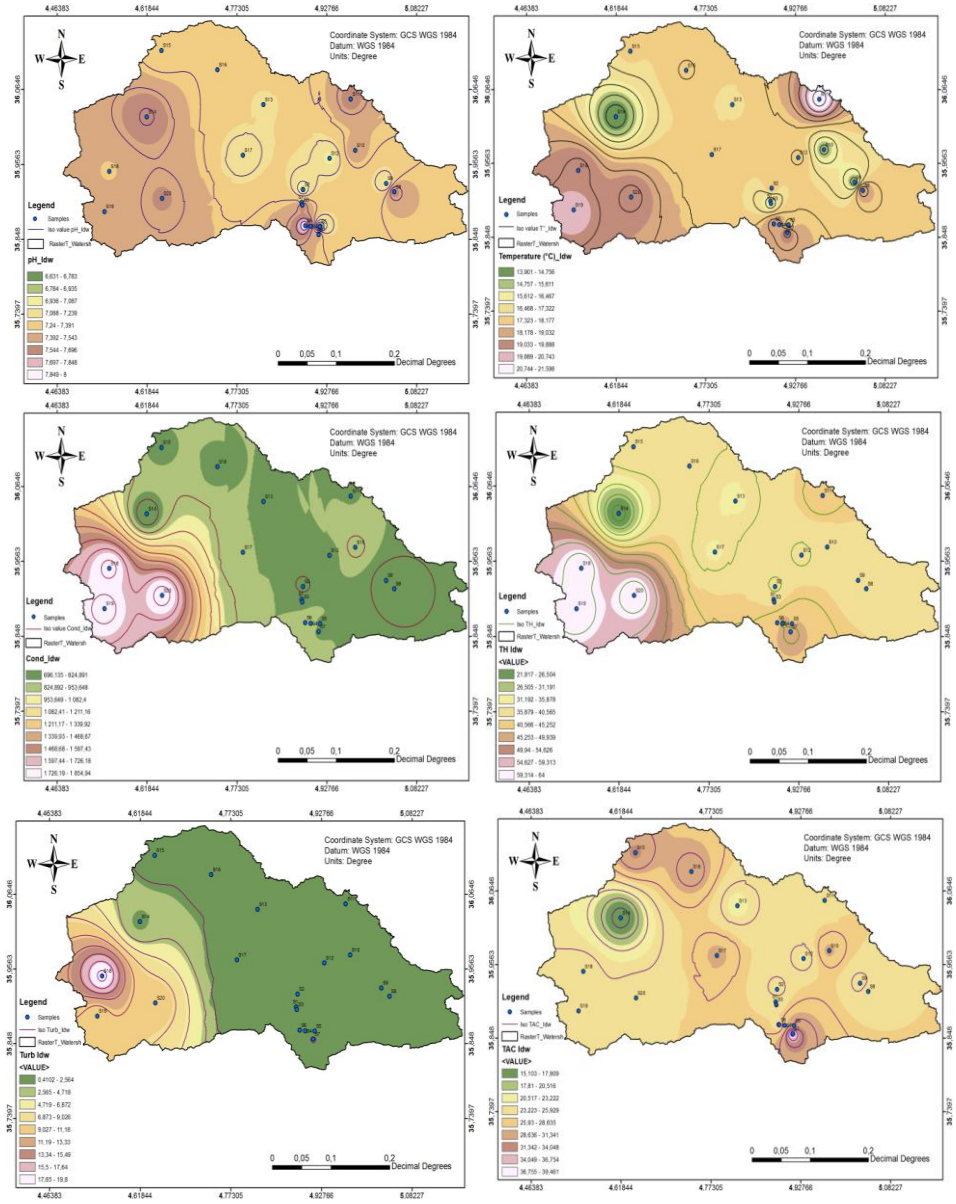
Coordinate System: GCS WGS 1984
Datum: WGS 1984
Units: Degree
Legend
pH_Idw
Temperature (°C)_Idw
Cond_Idw
TH Idw
Turb Idw
TAC Idw
Decimal Degrees

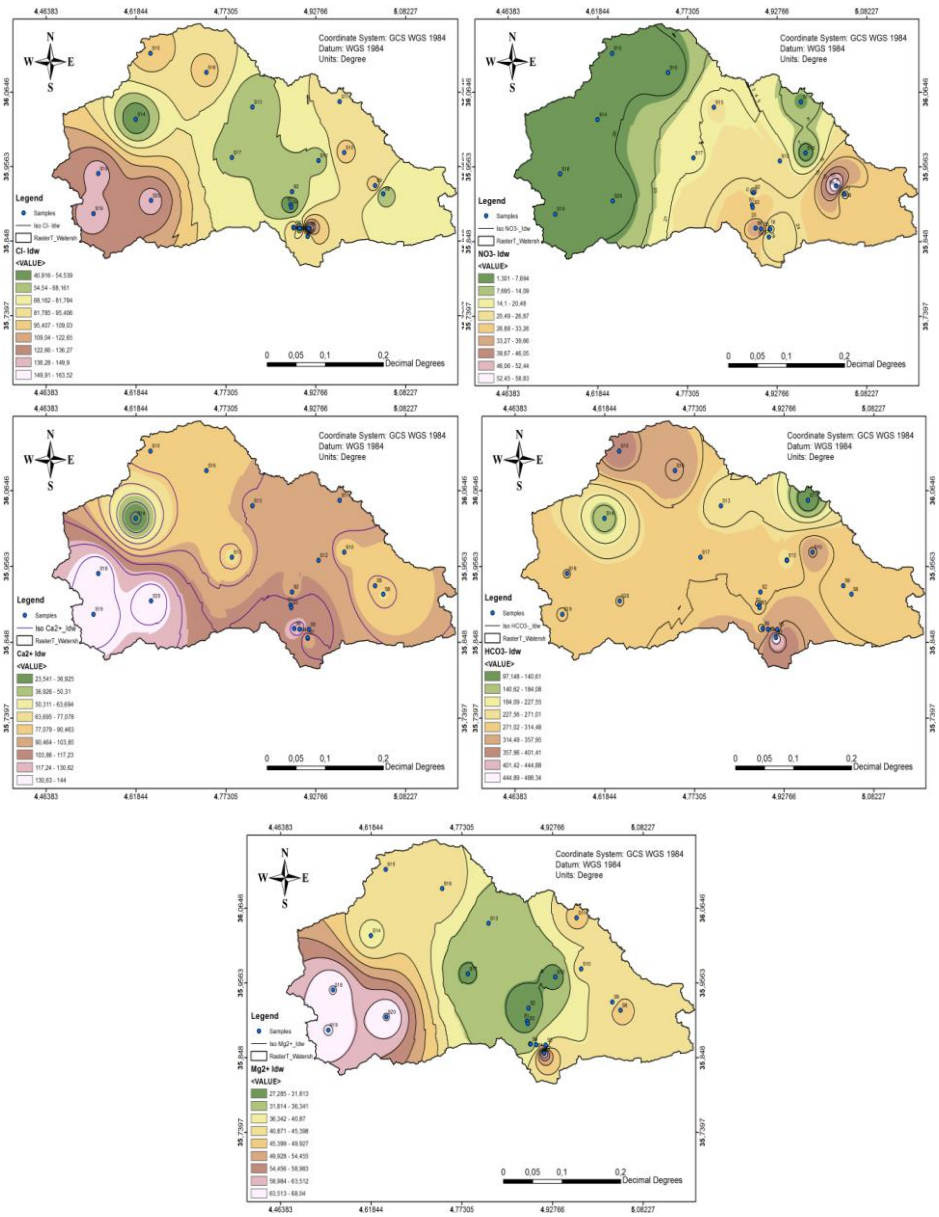

Fig. 4. Maps showing the spatial distribution of groundwater quality parameters (pH, T°, EC, TH, Turbidity, TAC, Cl^-, NO_3^-, HCO_3^-, Ca+2, and Mg+2) in K'sob watershed

Spatio-Temporal Variation of Water Quality Index

Understanding the spatial and temporal variations in water quality is paramount for sustainable water resource management and environmental protection. This study presents a comprehensive analysis of groundwater quality dynamics through a detailed Water Quality Index (WQI) evaluation conducted in K'sob watershed during two distinct periods: 2022 and 2024.

Table 5. Groundwater classification based on WQI

Number	WQI 2022	Classification	WQI 2024	Classification
S1	53,46	Good water	48,16	Excellent water
S2	49,62	Excellent water	42,21	Excellent water
S3	58,11	Good water	47,98	Excellent water
S4	53,29	Good water	55,23	Good water
S5	61,03	Good water	65,32	Good water
S6	57,84	Good water	55,02	Good water
S7	224,05	Very poor water	223,51	Very poor water
S8	88,02	Good water	82,95	Good water
S9	139,37	Poor water	129,02	Poor water
S10	152,02	Poor water	160,32	Poor water
S11	62,81	Good water	66,36	Good water
S12	52,37	Good water	45,36	Excellent water
S13	50,29	Good water	46,98	Excellent water
S14	192,72	Poor water	256,08	Very poor water
S15	83,08	Good water	194,44	Poor water
S16	82,35	Good water	81,23	Good water
S17	63,98	Good water	58,13	Good water
S18	1618,13	Unsuitable	1352,08	Unsuitable
S19	825,73	Unsuitable	741,25	Unsuitable
S20	859,67	Unsuitable	500,11	Unsuitable

Analysis of the Water Quality Index (WQI) results from the K'sob watershed reveals significant spatial and temporal variations during the monitoring period (2022-2024) (Figure 5). The WQI assessment highlighted a notable evolution in water quality distribution between 2022 and 2024. In 2022, only 5% of samples were of excellent quality, 60% good quality, 15% poor quality, 5% very poor quality, and 15% unsuitable for drinking purposes. By 2024, the proportion of samples with excellent quality increased to 25%, while those with good quality decreased to 35%. Samples with poor quality remained stable at 15%, those with very poor quality increased to 10%, and those unsuitable for drinking remained at 15%.

These data demonstrate a significant improvement in water quality at several sampling points: five sites (S1, S2, S3, S12, S13) were classified as "excellent water" in 2024, compared to only one site (S2) in 2022. Conversely, site S14 showed marked deterioration, changing from "poor water" (WQI = 192.72) to "very poor water" (WQI = 256.08), while site S15 also declined from the "good water" category to "poor water".

The deterioration observed at sites S14 and S15 can be attributed to localized anthropogenic pressures, particularly improper waste disposal practices and intensified urbani-

zation activities in these specific areas, which have introduced elevated levels of contaminants including nutrients and organic pollutants into the groundwater system. This interpretation is strongly supported by the elevated turbidity values observed at sites. Persistent water quality issues were observed at sites S7, S9, S10, S18, S19, and S20, with particularly concerning conditions at sites S18, S19, and S20, which maintained the "Unsuitable" classification throughout the study period despite some improvement in absolute WQI values.

The spatial distribution of WQI values highlights the influence of localized anthropogenic factor on groundwater quality. These results underscore the heterogeneous nature of groundwater quality in the watershed and emphasize the importance of targeted management interventions in severely affected areas (Brown et al., 1972; Ramakrishnaiah et al., 2009).

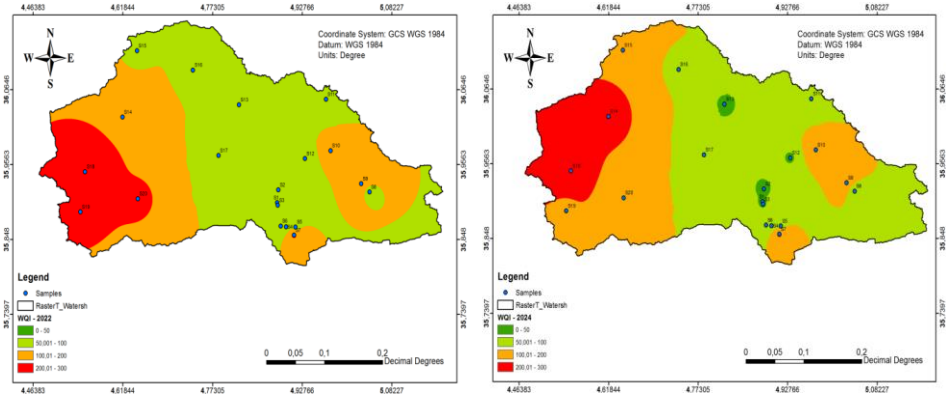

Fig. 5. Water quality index maps (2022 – 2024) of the study area

In the K'sob aquifer, correlation analysis revealed significant hydrogeochemical relationships (Table 6), indicating dominant mineral dissolution processes (Helena et al., 2000; Belkhiri et al., 2010). The substantial correlations between hardness parameters (TH, Ca^{2+}, Mg^{2+}) and conductivity suggest prevalent carbonate mineral weathering (Li et al., 2018), while temperature correlations with hardness parameters demonstrate temperature-dependent dissolution mechanisms. Notably, nitrate exhibited negative correlations with most parameters, suggesting distinct anthropogenic sources rather than natural mineral dissolution, potentially from agricultural activities or wastewater infiltration (Appelo and Postma, 2005; Zghibi et al., 2013). The strong relationship between conductivity and turbidity indicates suspended particles are predominantly ionic in nature (Todd and Mays, 2005).

Based on the lithological context of the K'sob watershed (Fig. 2), the overall correlation pattern suggests the aquifer interacts both with carbonate and evaporite lithologies (Hem, 1985). This geological framework offers essential insights into the groundwater geochemical evolution and potential contamination pathways in this semiarid watershed.

Table 6. Correlation matrix between groundwater quality parameters of K'sob aquifer

Parameter	T°	pH	Cond	Turb	TAC	TH	Ca^{++}	Mg^{++}	Cl^-	HCO_3^-	NO_3^-
T°	**1**										
pH	0,201	**1**									
Cond	0,466	0,173	**1**								
Turb	0,372	0,125	0,907	**1**							
TAC	0,328	-0,138	-0,044	-0,070	**1**						
TH	0,683	0,157	0,878	0,770	0,291	**1**					
Ca^{++}	0,578	0,062	0,696	0,526	0,152	0,853	**1**				
Mg^{++}	0,539	0,212	0,745	0,757	0,318	0,774	0,345	**1**			
Cl^-	0,362	-0,172	0,631	0,573	0,240	0,672	0,497	0,624	**1**		
HCO_3^-	0,058	-0,132	0,078	0,063	0,814	0,299	0,212	0,275	0,198	**1**	
NO_3^-	-0,253	-0,083	-0,445	-0,435	-0,129	-0,269	-0,023	-0,483	-0,385	0,025	**1**

Conclusion

This research presents a comprehensive assessment of groundwater quality in the K'sob watershed in eastern Algeria using an integrated methodological approach combining Water Quality Index (WQI) and Geographic Information System (GIS) techniques. The spatio-temporal analysis of groundwater quality parameters between 2022 and 2024 revealed significant variations in water quality across the study area, providing crucial insights for sustainable water resource management in this semi-arid region.

The WQI assessment demonstrated notable changes in water quality distribution over the two-year monitoring period. In 2022, only 5% of samples were classified as excellent quality, while by 2024, this proportion increased substantially to 25%, indicating localized improvements in groundwater conditions. Concurrently, the percentage of good quality samples decreased from 60% to 35%, suggesting potential deterioration in previously high-quality locations. The proportion of samples classified as poor quality remained constant at 15%, while very poor quality samples increased from 5% to 10%, and unsuitable samples remained steady at 15%. These temporal variations highlight the dynamic nature of groundwater quality in response to changing environmental and anthropogenic pressures.

Statistical analysis of eleven physicochemical parameters revealed significant spatial heterogeneity across the watershed. pH values indicated slightly alkaline conditions (mean: 7.37 ± 0.32) with uniform distribution, while electrical conductivity values ranged from 696 to 1855 µS/cm, remaining below regulatory limits but showing notable concentration in southern and southeastern areas. Total hardness exceeded recommended levels in approximately 15% of samples, correlating with elevated EC values and suggesting common hydrogeochemical processes related to carbonate mineral dissolution.

Correlation analysis revealed significant hydrogeochemical relationships among water quality parameters, with particularly strong positive correlations between electrical conductivity and turbidity (r=0.907), conductivity and total hardness (r=0.878), and total hardness with calcium (r=0.853) and magnesium (r=0.774). These relationships indicate dominant mineral dissolution processes within the aquifer system, consistent with the watershed's geological framework comprising carbonate and evaporite formations.

Notably, nitrate exhibited negative correlations with most parameters, suggesting distinct anthropogenic sources rather than natural mineral dissolution, potentially from agricultural activities or wastewater infiltration, as evidenced by the nitrate hotspot at site S9 exceeding WHO limits.

The spatial distribution maps generated through IDW interpolation in a GIS environment effectively visualized the heterogeneous nature of groundwater quality across the watershed, highlighting zones of particular concern that require targeted management interventions. Sites S18, S19, and S20 maintained their "unsuitable for drinking" classification throughout the study period, despite some improvement in absolute WQI values, indicating persistent water quality challenges in the southwestern discharge zone. Conversely, sites S14 and S15 showed marked deterioration, attributed to localized anthropogenic pressures including improper waste disposal and intensified urbanization activities.

The hydrogeological analysis revealed a dominant groundwater flow direction from east/northeast toward west/southwest, with primary recharge zones in eastern sectors and discharge areas in southwestern regions. The integration of geological mapping, piezometric monitoring, and surface drainage analysis validated the conceptual hydrogeological model and explained the observed water quality patterns in relation to aquifer characteristics and flow dynamics.

This study successfully demonstrates the effectiveness of combining WQI and GIS methodologies for comprehensive groundwater quality assessment and monitoring in semi-arid regions. The integrated approach provides a systematic framework for rapid spatial identification of water quality variations with respect to drinking water suitability. The findings provide valuable insights for water resource managers and policymakers in developing sustainable groundwater management strategies for the K'sob watershed and similar hydrogeological settings.

Future research should focus on identifying specific anthropogenic and geogenic factors influencing the observed water quality patterns, particularly investigating the sources of contamination at persistently problematic sites. Development of targeted remediation measures for severely affected areas, implementation of protection strategies for recharge zones, and establishment of regular monitoring protocols are essential for long-term water resource sustainability. Additionally, continued spatio-temporal monitoring is crucial to track long-term trends, evaluate the effectiveness of any implemented management interventions, and adapt management strategies to changing environmental conditions in this climatically sensitive region.

Conflicts of Interest: The authors declare no conflict of interest.

References

Ali, S., Verma, S., Agarwal, M.B., Islam, R., Mehrotra, M., Kumar Deolia, R., Kumar, J., Singh, S., Mohammadi, A. A., Raj, D., Kumar Gupta, M., Dang, P., & Fattahi, M. (2024). Groundwater quality assessment using water quality index and principal component analysis in the Achnera block, Agra district, Uttar Pradesh, Northern India. *Scientific Reports, 14*, Article 5381. https://doi.org/10.1038/s41598-024-56056-8

APHA (2005). *Standard methods for the examination of water and wastewater*. American Public Health.

Appelo, C.A.J., & Postma, D. (2005). *Geochemistry, Groundwater and Pollution (2nd ed.)*. Amsterdam: Balkema Publishers.

Bahrami, A., Bahrami, M., & Haghani, E. (2024). Groundwater quality assessment for potable using WQI and GIS technology in the south of Iran. *Sustainable Water Resources Management, 10*, Article 177. https://doi.org/10.1007/s40899-024-00978-8

Benkadja, R., Hattab, A., Mahdaoui, N., & Zehar, C. (2012). Assessment of soil losses and siltation of the K'sob hydrological system (semiarid area—East Algeria). *Arabian Journal of Geosciences, 6*(10), 3959-3968. https://doi.org/10.1007/s12517-012-0653-z

Bourmada, A., Khammar, H., Ramzi, H., Chaffai, A., Bouchema, N., & Hamida, B. (2024). Integrated assessment of groundwater quality in Algeria's Souk Ahras region: Implications for sustainable and management water for drinking and irrigation purpose. *Desalination and Water Treatment, 320*, Article 100827. https://doi.org/10.1016/j.dwt.2024.100827

Brown, R.M., McClelland, N.I., Deininger, R.A., & Tozer, R.G. (1970). A water quality index: do we dare? *Water Sewage Works, 117*, 339-343.

Chabuk, A., Al-Madhlom, Q., Al-Maliki, A., Al-Ansari, N., Hussain, H.M., & Laue, J. (2020). Water quality assessment along Tigris River (Iraq) using water quality index (WQI) and GIS software. *Arabian Journal of Geosciences, 13*, Article 654. https://doi.org/10.1007/s12517-020-05575-5

Chaurasia, A.K., Pandey, H.K., Tiwari, S.K., Prakash, R., Pandey, P., & Ram, A. (2018). Groundwater quality assessment using water quality index (WQI) in parts of Varanasi district, Uttar Pradesh, India. *Journal of the Geological Society of India, 92*, 76-82.

Chatterjee, C., & Raziuddin, M. (2002). Determination of Water Quality Index(WQI) of a degraded river in Asansol industrial area (West Bengal). *Nature, Environment and Pollution Technology, 1*(2), 181-189

Chen, F.W., & Liu, C.W. (2012). Estimation of the spatial rainfall distribution using inverse distance weighting (IDW) in the middle of Taiwan. *Paddy and Water Environment, 10*(3), 209-222. https://doi.org/10.1007/s10333-012-0319-1

ESRI (Environmental Systems Research Institute) (2018). *How IDW works. ArcGIS Pro Documentation*. https://pro.arcgis.com/en/pro-app/latest/tool-reference/3d-analyst/how-idw-works.htm

Faraji, H., & Shahryari, A. (2024). Assessment of groundwater quality for drinking, irrigation, and industrial purposes using water quality indices and GIS technique in Gorgan aquifer. *Desalination and Water Treatment, 320*, Article 100821. https://doi.org/10.1016/j.dwt.2024.100821

Fentie, A.Y., Mengistu, D.A., & Molla, G. (2024). Assessment of groundwater quality for drinking purpose using GIS based WQI methods, in Koga irrigation. *Water Science, 38*(1), 618-631. https://doi.org/10.1080/11104929.2024.2301357

Hem, J.D. (1985). *Study and Interpretation of the Chemical Characteristics of Natural Water*. U.S. Geological Survey Water-Supply.

Kanagaraj, G., Suganthi, S., Elango, L., & Magesh, N.S. (2019). Assessment of groundwater potential zones in Vellore district, Tamil Nadu, India using geospatial techniques. *Earth Science Informatics, 12*, 211-223. https://doi.org/10.1007/s12145-018-0363-5

Ketata-Rokbani, M., Gueddari, M., & Bouhlila, R. (2011). Use of geographical information system and Water Quality Index to assess groundwater quality in El Khairat Deep Aquifer (Enfidha, Tunisian Sahel). *Iranian Journal of Energy and Environment, 2*(2), 133-144.

Li, P., Wu, J., & Qian, H. (2018). Hydrochemical appraisal of groundwater quality for drinking and irrigation purposes and the major influencing factors: a case study in and around Hua County, China. *Arabian Journal of Geosciences, 11*, Article 350. https://doi.org/10.1007/s12517-018-3690-4

Lo, C.P., & Yeung, A.K. (2003). *Concepts and techniques of geographic information systems*. Prentice-Hall of India Pvt. Ltd, New Delhi.

Lu, G.Y., & Wong, D.W. (2008). An adaptive inverse-distance weighting spatial interpolation technique. *Computers & Geosciences, 34*(9), 1044-1055. https://doi.org/10.1016/j.cageo.2007.07.010

Masood, A., Aslam, M., Pham, Q.B., Khan, W., & Masood, S. (2022). Integrating water quality index, GIS and multivariate statistical techniques towards a better understanding of drinking water quality. *Environmental Science and Pollution Research, 29*, 26860-26876. https://doi.org/10.1007/s11356-021-17594-0

Milovanović, M. (2007). Water quality assessment and determination of pollution sources along the Axios/Vardar River, Southeastern Europe. *Desalination, 213*, 159-173. https://doi.org/10.1016/j.desal.2006.03.607

Ministère des Ressources en Eau, Algérie (2014). *Norme Algérienne NT 03-01 relative à la qualité des eaux destinées à la consommation humaine*. Ministère des Ressources en Eau, Algérie.

Mishra, P.C., & Patel, R.K. (2001). Study of the pollution load in the drinking water of Rairangpur, a small tribal dominated town of North Orissa. *Indian Journal of Environmental Ecoplan, 5*(2), 293-298.

Naik, S., & Purohit, K.M. (2001). Studies on water quality of river Brahmani in Sundargarh district, Orissa. Indian Journal of Environmental Ecoplan, 5(2), 397-402

Piyathilake, I.D.U.H., Udayakumara, E.P.N., Ranaweera, L.V., & Gunatilake, S.V. (2022). Modeling predictive assessment of carbon storage using InVEST model in Uva province, Sri Lanka. *Modeling Earth Systems and Environment, 8*, 2213-2223, https://doi.org/10.1007/s40808-021-01207-3

Pius, A., Rajeshwari, K., & Lebel, L. (2012). Hydrochemical characteristics and groundwater quality assessment of coastal aquifers, South India. *Environmental Monitoring and Assessment, 184*(5), 2683-2696. https://doi.org/10.1007/s11270-011-1027-y

Ram, A., Tiwari, S.K., Pandey, H.K., et al. (2021). Groundwater quality assessment using water quality index (WQI) under GIS framework. *Applied Water Science, 11*, 46. https://doi.org/10.1007/s13201-021-01376-7

Ramakrishnaiah, C.R., Sadashivaiah, C., & Ranganna, G. (2009). Assessment of water quality index for the groundwater in Tumkur Taluk, Karnataka State, India. *E-Journal of Chemistry, 6*(2), 523-530. https://doi.org/10.1155/2009/757424

Ramesh, K., & Elango, L. (2006). Groundwater quality assessment in Tondiar basin. *Indian Journal of Environmental Protection, 26*, Article 497.

Ravikumar, P., Somashekar, R., & Angami, M. (2011). Hydrochemistry and evaluation of groundwater suitability for irrigation and drinking purposes in the Markandeya River basin, Belgaum District, Karnataka State, India. *Environmental Monitoring and Assessment, 173*, 459-487. https://doi.org/10.1007/s10661-010-1399-2

Sadat-Noori, S.M., Ebrahimi, K., & Liaghat, A.M. (2014). Groundwater quality assessment using the Water Quality Index and GIS in Saveh-Nobaran aquifer, Iran. *Environmental Earth Sciences, 71*, 3827-3843. https://doi.org/10.1007/s12665-013-2770-8

Sadat-Noori, S.M., Ebrahimi, K., & Sriyoon, S. (2014). Groundwater quality and hydrochemical characteristics in the Lenjan Plain, Isfahan, Iran. *Applied Water Science, 4*(3), 249-258. https://doi.org/10.1007/s13201-014-0215-5

Shepard, D. (1968). A two-dimensional interpolation function for irregularly-spaced data. *Proceedings of the 1968 23rd ACM National Conference* (pp. 517-524). https://doi.org/10.1145/800186.810616

Srinivasamoorthy, K., Chidambaram, M., Prasanna, M.V., Vasanthavigar, M., Peter, A.J., & Anandhan, P. (2008). Identification of major sources controlling groundwater chemistry from a hard rock terrain—a case study from Mettur taluk, Salem district, Tamilnadu, India. *Journal of Earth System Science, 117*(1), 49-58, https://doi.org/10.1007/s12040-008-0012-3

Standard Methods International (2018). *Standard Methods for the Examination of Water and Wastewater*. APHA-AWWA-WEF Publication.

Todd, D.K., & Mays, L.W. (2005). *Groundwater Hydrology (3rd ed.)*. John Wiley & Sons.

Umar, R., Ahmed, I., & Alam, F. (2009). Mapping groundwater vulnerable zones using modified DRASTIC approach of an alluvial aquifer in parts of Central Ganga Plain, Western Uttar Pradesh. *Journal of Geological Society of India, 73*, 193-201, https://doi.org/10.1007/s12594-009-0073-1

Webster, R., & Oliver, M. A. (2007). *Geostatistics for Environmental Scientists (2nd ed.)*. John Wiley & Sons Ltd. https://doi.org/10.1002/9780470517277

World Health Organization (2017). *Guidelines for drinking-water quality: Fourth edition incorporating the first addendum*. WHO Press.

Zghibi, A., Tarhouni, J., & Zouhri, L. (2013). Assessment of seawater intrusion and nitrate contamination on the groundwater quality in the Korba coastal plain of Cap-Bon (North-east of Tunisia). *Journal of African Earth Sciences, 87*, 1-12. https://doi.org/10.1016/j.jafrearsci.2013.07.009